

Physicochemical and Immunocytochemical Analysis of the Aryl Hydrocarbon Receptor Nuclear Translocator: Characterization of Two Monoclonal Antibodies to the Aryl Hydrocarbon Receptor Nuclear Translocator

NORMAN G. HORD and GARY H. PERDEW

Department of Foods and Nutrition, Purdue University, West Lafayette, Indiana 47904

Received April 21, 1994; Accepted July 11, 1994

SUMMARY

The aryl hydrocarbon receptor nuclear translocator (Arnt) is a basic helix-loop-helix transcription factor that heterodimerizes with the aryl hydrocarbon receptor to mediate signal transduction pathways inducible by 2,3,7,8-tetrachlorodibenzo-*p*-dioxin and other planar aromatic hydrocarbons. Monoclonal antibodies (MAbs) have been raised against a carboxyl-terminal 19-amino acid peptide hapten (MAb 2B10) and against a carboxyl-terminal 378-amino acid polypeptide-staphylococcal Protein A fusion protein (MAb 4G9) of Arnt and their characterization is described. Western blot experiments show that both MAbs specifically cross-react with an ~85-kDa band in cytosol prepared from COS-7 cells transfected with the full length human Arnt cDNA pBMSNeo-D24-1 and in Hepa 1c1c7 cytosol but not in Arnt-deficient Hepa 1-C4 mutant cytosol. Velocity sedimentation of Hepa 1c1c7 cytosol on sucrose gradients and Superose 6 gel permeation chromatography were used to estimate the sedimentation

coefficient, Stokes radius, and relative molecular mass of Arnt as ~3.6–4.1 S, 6.8 nm, and 101–115 kDa, respectively. These results indicate that Arnt probably exists in monomeric form in Hepa 1c1c7 cytosolic extracts. Laser scanning confocal microscopy and indirect immunofluorescence microscopy revealed Arnt to be distributed throughout the non-nucleolar portion of the nucleus of Hepa 1c1c7, VT{2} (Hepa 1-C4T mutant cell line deficient in Arnt function and stably transfected with pBMSNeo D24-1, expressing the full length human Arnt cDNA), and HeLa cells. The establishment of the nuclear localization of Arnt in human and murine cell lines shown here indicates that its nuclear localization may be conserved across species. Immunofluorescence analysis of Arnt in three cell lines using two MAbs (to distinct epitopes) provides evidence that suggests that the aryl hydrocarbon receptor heterodimerizes with Arnt in the nucleus.

The Arnt is an ~87-kDa bHLH transcription factor that is required for proper functioning of the AhR, due to its heteromeric association with Arnt to form a DNA-binding heterodimer (1–3). The DNA-binding properties of the AhR-Arnt heterodimer are thought to mediate the biological effects of exposure to the environmental contaminant TCDD (dioxin) or other planar aromatic hydrocarbons such as benzo(*a*)pyrene and 3-methylcholanthrene (4). Among the biochemical and toxicological effects attributable to TCDD exposure in rodents are wasting syndrome, thymic atrophy, immunotoxicity, developmental and reproductive toxicity, and site-specific tumor promotion. These effects vary greatly by species, strain, and sex

of the animal examined (5). Conserved protein motifs in Arnt and AhR provide clues concerning their biological functions. Both Arnt and AhR display significant sequence similarity to a family of transcriptional regulators that includes the nucleus-localized *Drosophila* regulatory proteins Per and Sim (5–7). Referred to as the PAS protein family, these proteins share two structural domains important in mediating protein-protein and protein-DNA interactions (6). The primary region of sequence similarity is the PAS domain, which lies near the amino terminus and encompasses 200–350 amino acids (4). This domain consists of two 51-amino acid repeats and was discovered in Per and Sim (8). The PAS domain of Per has been shown to mediate heterodimerization between certain members of the PAS protein family in *in vitro* coimmunoprecipitation experiments (6). Interestingly, the AhR contains amino acid se-

This work was supported in part by National Institute of Environmental Health Sciences Grant ES04869. This is technical paper No. 14,182 of the Indiana Agricultural Experiment Station.

ABBREVIATIONS: Arnt, aryl hydrocarbon receptor nuclear translocator; MAb, monoclonal antibody; bHLH, basic helix-loop-helix; AhR, aryl hydrocarbon receptor; TCDD, 2,3,7,8-tetrachlorodibenzo-*p*-dioxin; Per, period; Sim, single-minded; PAS, Per/Arnt/AhR/Sim; LRSC, lissamine rhodamine sulfonyl chloride; PVDF, polyvinylidene difluoride; HPLC, high performance liquid chromatography; KLH, keyhole limpet hemocyanin; LSCM, laser scanning confocal microscopy; NLS, nuclear localization sequence(s); hsp90, 90-kDa heat shock protein; BSA, bovine serum albumin; PBS, phosphate-buffered saline; ELISA, enzyme-linked immunosorbent assay; SDS, sodium dodecyl sulfate; PAGE, polyacrylamide gel electrophoresis; DMSO, dimethylsulfoxide; MOPS, 3-(*N*-morpholino)propanesulfonic acid; MES, 2-(*N*-morpholino)ethanesulfonic acid.

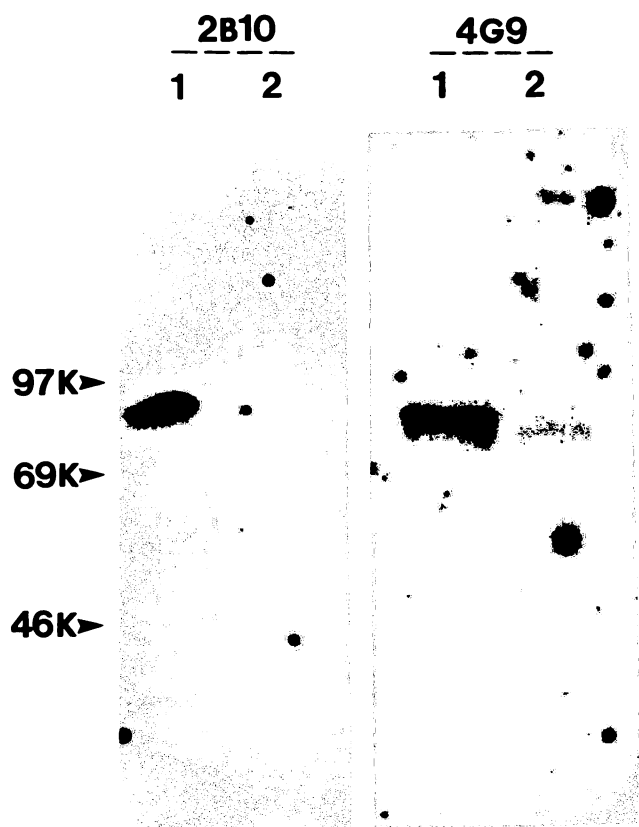


Fig. 1. Immunoblotting of COS cell extracts. COS-2 (lanes 1) and COS-1 (lanes 2) cell extracts were isolated and 150 μ g of protein/lane were separated by SDS-PAGE and electroblotted onto PVDF membranes. The protein blots were screened with either MAB 2B10 supernatant (0.1 \times) or affinity-purified MAB 4G9 (1 μ g/ml) and visualized with radioiodinated goat anti-mouse IgG, as detailed in Materials and Methods.

quences indicative of a ligand-binding hydrophobic pocket in this domain (9). The second region of similarity, oriented just amino-terminal to the PAS domain, is the bHLH domain. It is found in all known PAS proteins except Per (10). As in other bHLH proteins, the basic region is thought to mediate DNA binding, whereas the helix-loop-helix region acts as a dimerization surface (4). Acting in concert, the respective bHLH and PAS domains may provide primary and secondary dimerization domains as well as a DNA binding domain, in a manner similar to that of the bHLH-leucine zipper domains of the well characterized heteromeric partners Myc/Max/Mad and MyoD/E2A (2, 11).

Arnt was cloned from human cDNA sequences capable of restoring *CYP1A1* inducibility after TCDD treatment in a mutant Hepa 1c1c7 cell line defective in *CYP1A1* gene expression (7, 12). It has since been demonstrated that both the ligand-activated AhR and Arnt bind directly to the DNA sequences known as dioxin-responsive elements in the 5' regulatory region of the *CYP1A1* gene (1, 2, 7). This heterodimer has also been identified as the 6 S liganded form of the AhR complex induced by TCDD treatment in dioxin-responsive cell lines (13, 14). The formation of this 6 S, DNA-binding heterodimer has been shown to require ligand binding to the cytosolic 9 S form of the AhR (1, 7). The complete composition of the 9 S AhR complex has not been established. Like steroid hormone receptors such as the glucocorticoid receptor, hsp90 is bound

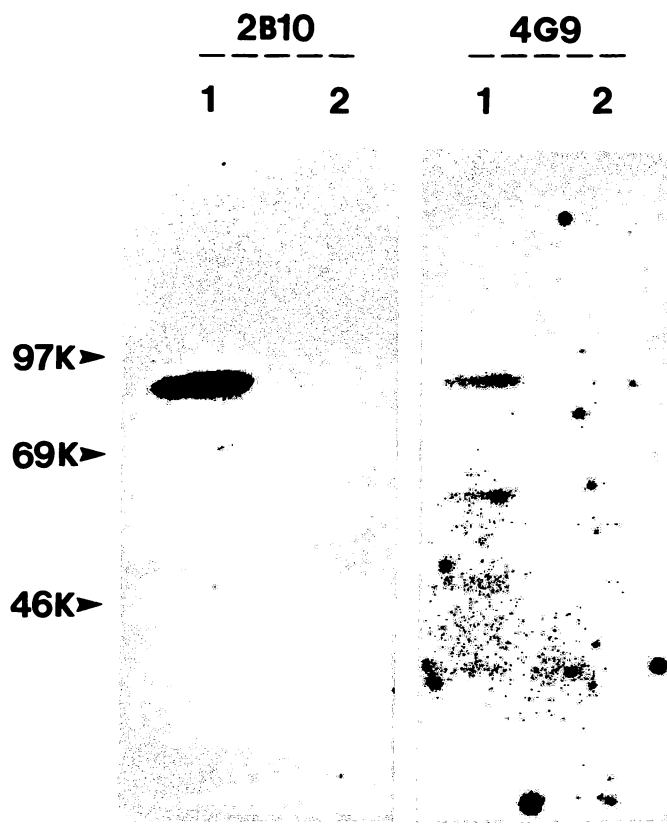


Fig. 2. Immunoblotting of Hepa 1c1c7 and Hepa 1-C4 cell extracts. Hepa 1c1c7 (lanes 1) and Hepa 1-C4 (lanes 2) cell extracts were isolated and 100 μ g of protein/lane were separated by SDS-PAGE and electroblotted onto PVDF membranes. The Western blots were screened with either MAB 2B10 supernatant (0.1 \times) or affinity-purified MAB 4G9 (1 μ g/ml) and visualized with radioiodinated goat anti-mouse IgG, as detailed in Materials and Methods.

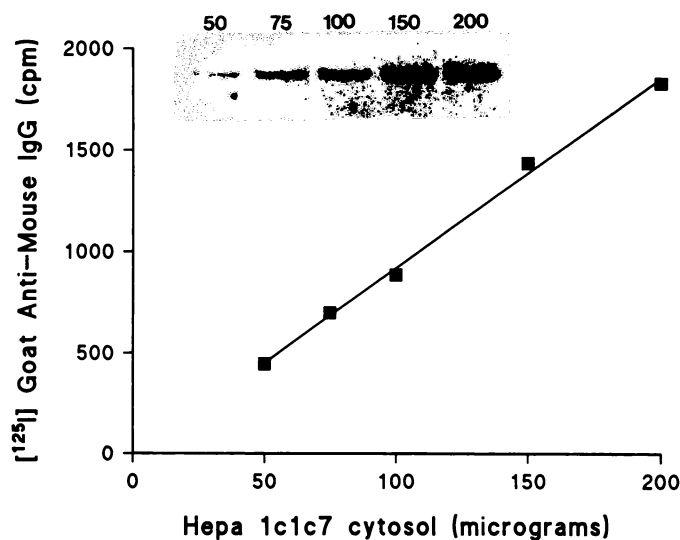


Fig. 3. Sensitivity of detection of MAB 2B10. Hepa 1c1c7 cytosol (50, 75, 100, 150, or 200 μ g/lane) was separated by SDS-PAGE, electroblotted, and screened with MAB 2B10 and ¹²⁵I-goat anti-mouse IgG Fc fragment antibodies. Radioactive bands were excised and counted in a Packard Cobra II γ counter. Resultant values were plotted versus protein concentration, and linear regression analysis was performed ($r^2 = 0.99$).

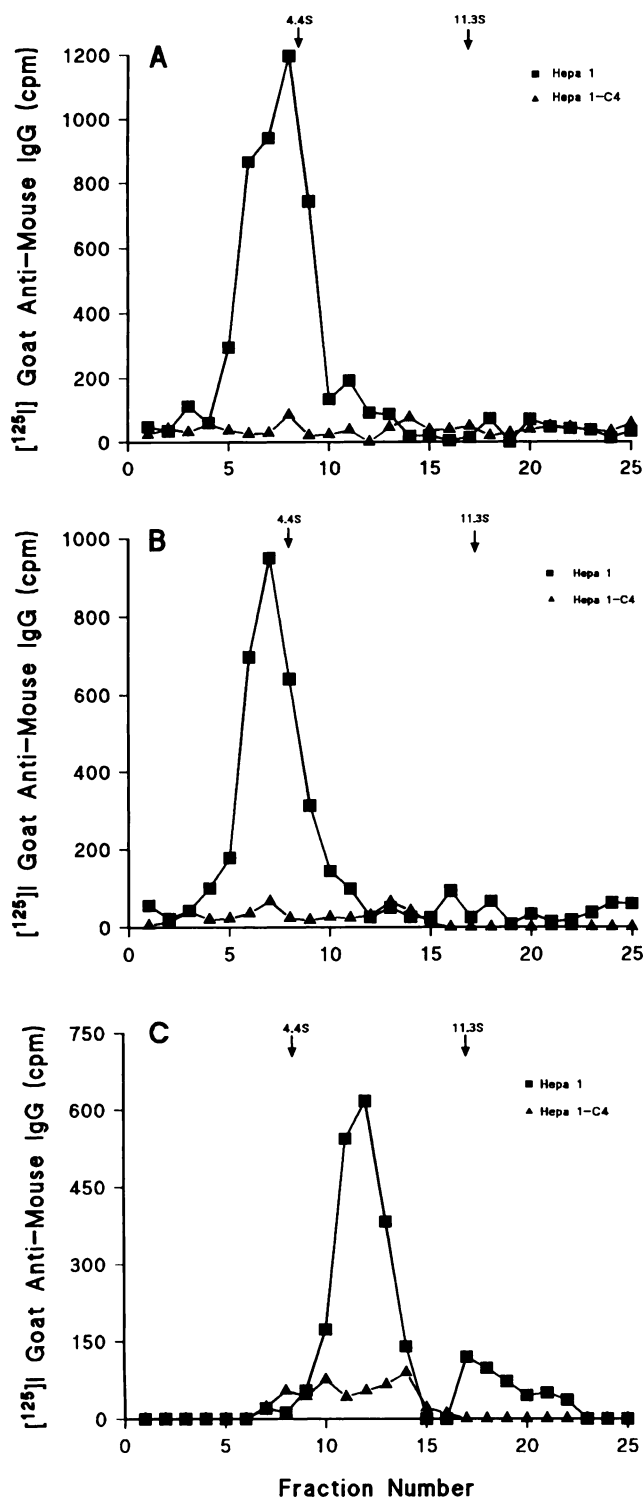


Fig. 4. Velocity sedimentation of Arnt from Hepa 1c1c7 cytosolic and nuclear protein in sucrose gradients and comparison of moderate and high ionic strength conditions. A, Cytosol samples were brought to 500 mM NaCl using a concentrated NaCl solution before being layered onto 5.1-ml 10–30% sucrose gradients prepared in MENG buffer containing 500 mM NaCl. B, Samples were brought to 150 mM before being layered onto 5.1-ml 10–30% sucrose gradients prepared in MENG buffer containing 150 mM. C, Nuclear extract from TCDD-treated cells was layered onto 5.1-ml sucrose gradients prepared in MENG buffer containing 500 mM NaCl. Gradient fractions were precipitated with acetone, separated by SDS-PAGE, electroblotted onto membranes, and screened with MAb 2B10 and 125 I-goat anti-mouse IgG Fc fragment antibodies. Radioactive bands

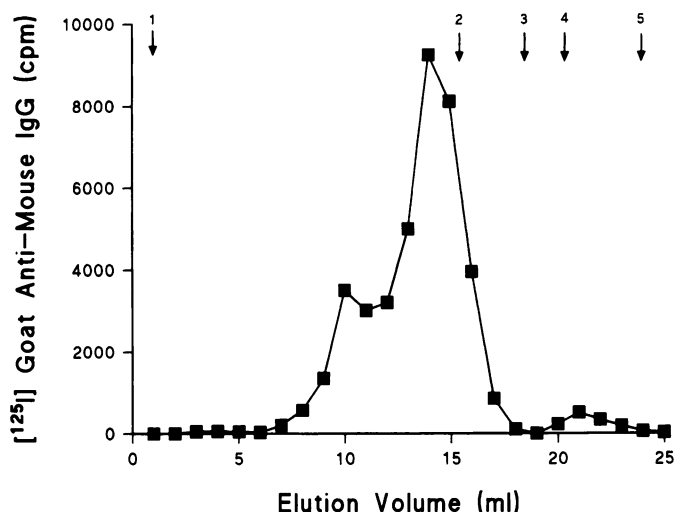


Fig. 5. Gel filtration of Arnt. Hepa 1c1c7 cytosol (6 mg/ml) and protein standards were chromatographed on a Superose 6 column equilibrated in MENG buffer with either 150 mM NaCl or 500 mM NaCl. Fractions were separated by SDS-PAGE, electroblotted, and screened with MAb 2B10 and 125 I-goat anti-mouse IgG Fc fragment antibodies. Radioactive bands were excised, counted in a Packard Cobra II γ counter, and plotted. The Superose 6 column was calibrated with protein standards of known Stokes radius, as follows: thyroglobulin (1), 8.5 nm; apoferritin (2), 6.1 nm; alcohol dehydrogenase (3), 4.5 nm; BSA (4), 3.6 nm; and carbonic anhydrase (5), 2.01 nm.

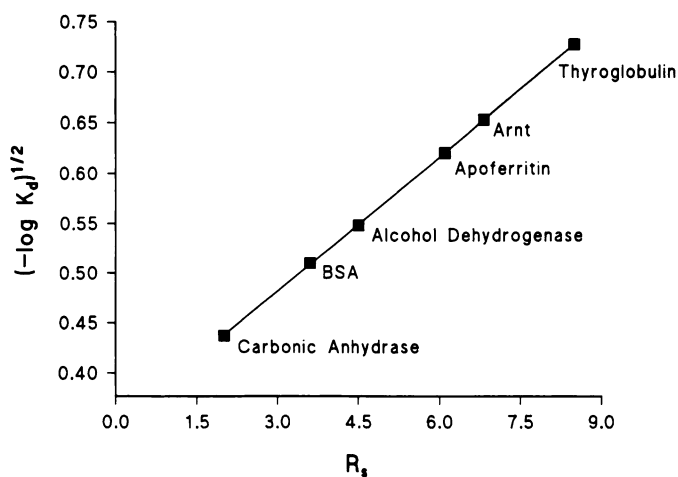


Fig. 6. Determination of the Stokes radius of Arnt. Linear regression analysis of the $(-\log K_d)^{1/2}$ values and Stokes radii (R_s) of the protein standards is displayed. The Stokes radius of Arnt was determined by plotting the calculated $(-\log K_d)^{1/2}$ value on the standard curve.

to the unliganded AhR (15). The mechanism of transformation of the 9 S complex to the 6 S complex is not completely understood. However, certain components of this pathway have been delineated. Several workers have shown that a ligand-dependent dissociation of hsp90 occurs before association of the ligand-binding subunit of the AhR with Arnt, before binding to dioxin-responsive elements (9, 16, 17). Others have demonstrated that Arnt is not a component of the 9 S AhR complex (1, 16).

were excised and counted in a Packard Cobra II γ counter. BSA (4.4 S) and catalase (11.3 S) were used to estimate molecular sizes, in a separate sucrose gradient.

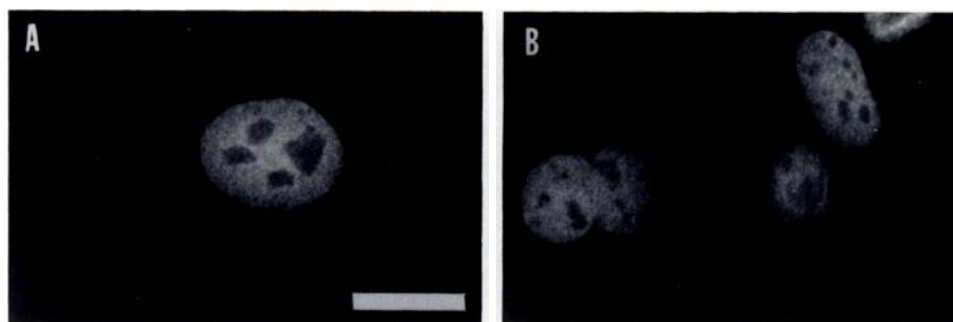


Fig. 7. LSCM micrographs of Arnt in Hepa 1c1c7 cells. Cells were prepared as described in Materials and Methods. A, Hepa 1c1c7 cells sequentially incubated with affinity-purified anti-Arnt MAB 4G9 (490 µg/ml) and goat anti-mouse IgG conjugated to LRSC; B, cells sequentially incubated with affinity-purified anti-Arnt MAB 4G9 and the same secondary antibody as in A, after 1-hr treatment with 1 nM TCDD. Bar, 10 µm.

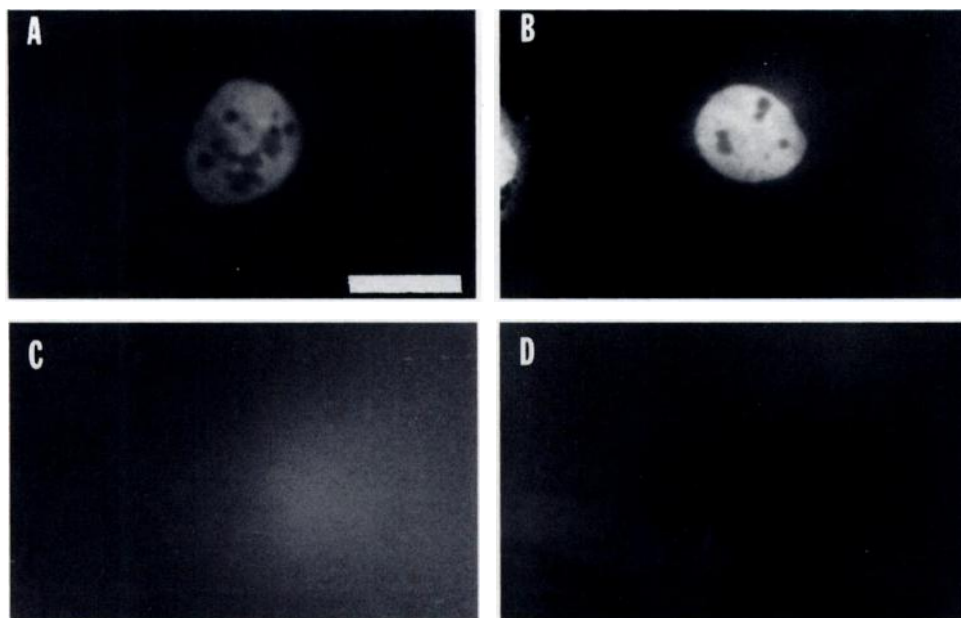


Fig. 8. Indirect immunofluorescence micrographs of Arnt in VT{2} cells. Cells were prepared as described in Materials and Methods. A, VT{2} cells sequentially incubated with affinity-purified anti-Arnt MAB 4G9 (490 µg/ml) and goat anti-mouse IgG conjugated to LRSC; B, cells sequentially incubated with affinity-purified anti-Arnt MAB 4G9 and the same secondary antibody as in A, after 1-hr treatment with 1 nM TCDD; C and D, cells incubated with mouse IgG1 or no primary antibody, respectively, with the same secondary antibody as in A. Bar, 10 µm.

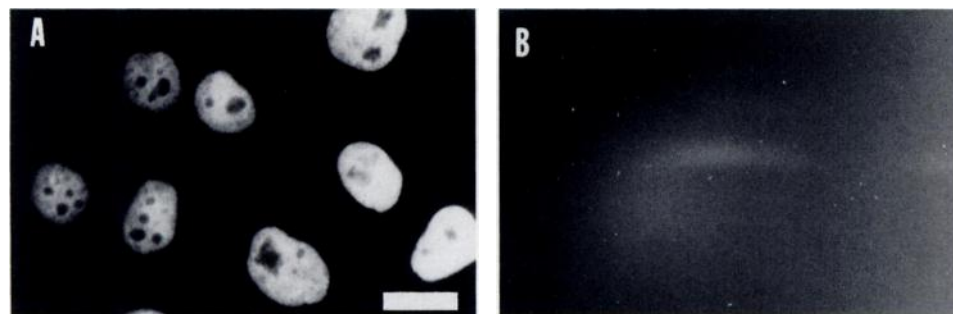


Fig. 9. Indirect immunofluorescence micrographs of Arnt in HeLa cells. Cells were prepared as described in Materials and Methods. A, HeLa cells sequentially incubated with affinity-purified anti-Arnt MAB 4G9 (490 µg/ml) and goat anti-mouse IgG conjugated to LRSC; B, cells incubated with mouse IgG1 and the same secondary antibody as in A. Bar, 10 µm.

A hypothetical model has been proposed to explain the role of Arnt in TCDD-mediated, AhR-dependent, signal transduction (2, 18). This model suggests that Arnt binds the ligand-activated ligand-binding subunit of the AhR in the cytoplasm after dissociation of hsp90, facilitating the nuclear translocation of the heterodimer (1, 2). Whitelaw *et al.* (16) have functionally reconstituted the DNA-binding phenotype in AhR nuclear translocation-deficient (nt⁻) mutant cell cytosol, using 4–5 S cytosolic extracts from Hepa 1c1c7 cells. These data suggest that Arnt may play an active role in recruiting the ligand-binding subunit of the AhR into the nucleus (16, 18). Alternately, data have been published suggesting that the transformation of the 9 S AhR complex to the 6 S, Arnt-containing species could occur in the nucleus (19, 20).

Several investigators have used velocity sedimentation on

sucrose gradients and gel permeation chromatography to establish the physicochemical characteristics of the AhR (14, 19, 21). A consensus summary of these results revealed that the unactivated cytosolic form of the AhR in mice and rats displays a sedimentation coefficient of 9 S and a Stokes radius of 7.2 nm (14, 19, 21). In contrast, the ligand-activated nuclear form of the AhR complex has a sedimentation coefficient of 6 S and a Stokes radius of 6.8 nm (14, 19, 21). Estimates of relative molecular mass based on these data are 270 kDa and 176 kDa for the 9 S and 6 S forms of the AhR, respectively. Upon prolonged exposure to high-salt buffer, a third form of the AhR is produced, possessing a sedimentation coefficient of 4.9S, a Stokes radius of 5 nm, and an estimated molecular mass of 104 kDa (14, 22). This species is believed to be the monomeric ligand-binding subunit of the AhR. In this report we use similar techniques to study the physicochemical properties of Arnt.

The goal of this work was to generate two MAbs to distinct epitopes in Arnt, which would yield tools applicable to a variety of experimental approaches. These MAbs were used in an immunofluorescence assay in Hepa 1c1c7 cells to examine the intracellular localization of Arnt in control and TCDD-treated mouse hepatoma and human epithelial cell lines. The utilization of immunofluorescence techniques avoids the problem of compartmental redistribution of proteins resulting from cell homogenization (4, 23). We have also used these MAbs to examine the sedimentation behavior of Arnt in sucrose gradients and gel permeation chromatography, to determine its physicochemical properties in Hepa 1c1c7 cells. The elucidation of these properties should shed light on the role of Arnt in AhR-mediated signal transduction.

Materials and Methods

Chemicals. LRSC-conjugated goat anti-mouse IgG, horseradish peroxidase-conjugated goat anti-mouse IgG, and goat anti-mouse IgG (Fc-specific) antibodies were purchased from Jackson ImmunoResearch Laboratories (West Grove, PA). Origen was purchased from IGEN (Rockville, MD). Fetal bovine serum was obtained from Hyclone Laboratories (Logan, UT). Sodium [125 I]iodide was obtained from DuPont (Boston, MA). Iodobeads were obtained from Pierce (Rockford, IL), and iodination of goat anti-mouse IgG (Fc specific) was carried out according to the method of Markwell (24). PVDF membranes were obtained from Millipore (Bedford, MA). Microculture plates (six-, 24-, and 96-well) were obtained from Corning Laboratory Sciences Co. (Corning, NY). All other reagents, unless otherwise noted, were obtained from Sigma Chemical Co. (St. Louis, MO).

Peptide and fusion protein synthesis and characterization. A synthetic peptide corresponding to the carboxyl-terminal sequence CNSYNNEFPDLTMFPFSE of the human Arnt protein (7) was prepared by the Purdue Peptide Synthesis Group using standard methods; an amino-terminal cysteine was added to the peptide to allow conjugation to activated protein. The peptide was purified by HPLC on a Vydac C_{18} reverse phase column (4.6×250 mm) and was coupled to KLH and BSA using the heterobifunctional cross-linking agent *N*-succinimidyl bromoacetate (25). The carboxyl-terminal Arnt polypeptide (amino acids 399–777)-staphylococcal Protein A fusion protein was expressed in *Escherichia coli* JM107, isolated, and purified on an IgG-Sepharose 6 Fast Flow affinity column (Pharmacia, Piscataway, NJ) by Dr. Herminio Reyes of the University of California, Los Angeles, Medical Center.

Immunization protocol, antibody production, and characterization. Female BALB/c mice (7–8 weeks of age) were purchased from The Jackson Laboratory. Three mice were given four subcutaneous injections of 100 μ g of the carboxyl-terminal 19-amino acid Arnt peptide-KLH conjugate or the carboxyl-terminal 378-amino acid-Protein A fusion protein. The first injection consisted of 0.3 ml of conjugate in PBS/Freund's complete adjuvant. The mice were boosted twice, at 4-week intervals, using the aforementioned dosage in Freund's incomplete adjuvant. One week after the third injection, 50 μ l of blood were obtained from the tail vein of each mouse and centrifuged at $3000 \times g$, and serum supernatant was stored at -20° in 0.02% sodium azide. For sera from mice injected with the 19-amino acid peptide-KLH conjugate, antibody titers were determined by indirect ELISA. Dot blots using the carboxyl-terminal Arnt-BSA conjugate as the antigen were used as an additional screening tool. Sera from mice injected with the fusion protein were screened against Hepa 1c1c7 cytosol separated by tricine-SDS-PAGE and blotted onto PVDF membranes in a Miniblotter unit. The spleen from the mouse producing serum with the highest antibody titer was used for subsequent production of hybridomas via fusion of spleen cells to the myeloma cell line SP2/O. Four weeks after the third injection of the immunogen and 4 days before fusion, the mouse was given an intraperitoneal injection of 100 μ g of immunogen in 0.3 μ l of

PBS. Immunized spleen cells and myeloma cells (SP2/O) were fused in the presence of polyethylene glycol. The fused cells were suspended in HAT medium (RPMI 1640 medium containing 10% fetal bovine serum, 10% Origen, 2 mM glutamine, 1 mM sodium pyruvate, 0.5 mM oxaloacetic acid, 0.01 mM hypoxanthine, 0.0016 mM thymidine, 0.0004 mM aminopterin, and 0.001 unit/ml insulin). Ten 96-well microtiter plates were seeded with 0.2 ml of the fusion mixture and incubated at 37° in 94% air/6% CO_2 . Microtiter plates were incubated undisturbed for 5 days before feeding with 100 μ l of HT medium (same as HAT medium but containing 5% Origen and no aminopterin). Fusion efficiency was assessed 7 days after fusion. ELISA screening of 50 μ l of supernatant was performed over a 3-day period from day 10 to day 12 after fusion. Indirect ELISA (for 19-amino acid peptide antibodies) or Western-blotted Hepa 1c1c7 cytosol (for fusion protein antibodies) was used to screen hybridoma supernatants. The carboxyl-terminal Arnt-BSA conjugate was dissolved in 0.01 M sodium carbonate buffer, pH 9.5, at a concentration of 100 ng/ml. One hundred microliters of this solution were added to each well of a 96-well microtiter plate and incubated overnight at 4° . Wells were washed three times by filling each well with 300 μ l of PBS, pH 7.4. Nonspecific binding was blocked by addition of 400 μ l of 1% BSA and incubation for 1 hr at room temperature. The wells were then washed two times with PBS, pH 7.4. Fifty microliters of microtiter plate supernatant were added to the wells and incubated for 1 hr at 37° . Duplicate wells of control mouse serum were used as negative controls. Unbound antibody was removed by washing five times with 300 μ l of 0.05% Tween 20 in PBS, pH 7.4. Fifty microliters of goat anti-mouse serum-peroxidase conjugate diluted 1/500 in PBS were then added to each well and incubated for 1 hr at 37° . The plate was then washed five times with 300 μ l of 0.05% Tween 20 in PBS, pH 7.4. Bound peroxidase was determined with 100 μ l of 2'-azino-bis(3-ethylbenzthiazoline-6-sulfonic acid) as a substrate. Positive wells were determined by visual inspection of color change. Cultures exhibiting the most intense color change were cloned by limiting dilution at five cells/well and were expanded in HT medium. Stabilized positive cell lines from the second cloning were cloned at one cell/well, expanded, and stored in liquid nitrogen. Positive wells were confirmed using peroxidase-linked immunostaining of PVDF Western blots prepared from SDS-PAGE gels of cytosol from three cell lines. The three cell lines used to prepare cytosol were COS-7 (nontransfected cells), pBMSNeo D24-1 (COS-7 cells transfected with expression vector containing full length ARNT cDNA), and pBM5Neo ZAP 56 (COS-7 cells transfected with expression vector containing Arnt cDNA with 163 amino acids missing from the carboxyl terminus). These cell lines are referred to here as COS-1, COS-2, and COS-3, respectively. Antibody isotype was determined using a Hyclone MAb subtyping kit (EK-5050; Hyclone Laboratories, Logan, UT). The carboxyl-terminal peptide-KLH-induced MAb was designated 2B10 and the carboxyl-terminal fusion protein-induced MAb was designated 4G9.

Mice were primed for antibody production in ascites by an intraperitoneal injection of 0.3 ml of Freund's incomplete adjuvant. After 24 hr, 2×10^7 hybridoma cells, diluted in 300 μ l of RPMI 1640 medium, were injected intraperitoneally. Abdominal swelling became evident in mice injected with 4G9 hybridomas but not 2B10 hybridomas. After 10 days, ascitic fluid was collected every 3 days (a total of three times) and the fluid was pooled. The 4G9 ascitic fluid was diluted 4-fold with buffer A (25 mM MES, pH 6) and dialyzed against buffer A overnight at 4° . The ascites was clarified for HPLC as described (26). The ascites was applied to a Versa-Ten (7.75- \times 100-mm) ABx HPLC column (J.T. Baker, Phillipsburg, NJ) equilibrated in buffer A, at a flow rate of 1 ml/min. After the unabsorbed protein was washed through with a linear 50-min gradient of 0–100%, 500 mM sodium phosphate, pH 6.8, was applied. The IgG peak fractions were pooled, the protein concentration was determined, and 1 mg/ml BSA was added, followed by dialysis against PBS. The 2B10 supernatant was used at $0.1\times$ concentration. Expansion of hybridoma cell line 2B10 for supernatant production was carried out in HT medium described above.

Cell culture. Hepa 1c1c7, VT[2], C4, and HeLa cells were grown in

α -minimum essential medium containing 5% fetal bovine serum, 100 IU/ml of penicillin, and 0.1 mg/ml streptomycin, at 37° in 94% air/6% CO₂. VT{2} cells had 0.04% geneticin added to maintain selection of stable transfectants. Treatment of cells with TCDD (diluted in DMSO) was carried out in 75-mm² culture flasks or on sterile slides at about 80% cell confluency. For TCDD treatment, a maximum of 0.05% DMSO (control) or TCDD solubilized in DMSO was added to the medium. The cells were harvested using trypsin/EDTA and washed with ice-cold PBS. The washed cells were homogenized in MENG buffer (25 mM MOPS, 1 mM EDTA, 0.02% sodium azide, 10% glycerol, pH 7.5) with 15 strokes in a Dura-Grind Dounce tissue grinder (Wheaton Instruments, Milville, NJ). The cell homogenate was centrifuged at 1000 × *g* for 15 min, and the supernatant was removed and centrifuged at 100,000 × *g* for 30 min. The 1000 × *g* pellet (nuclear pellet) was resuspended and washed three times with MENG buffer. The nuclear pellet was then resuspended in 300 μ l of MENG buffer plus 500 mM NaCl and was gently shaken at 4° for 1 hr. Nucleus-associated membranes were removed from the nuclear pellet by centrifugation at 100,000 × *g* for 1 hr.

Separation, immunoblotting, and detection of Arnt. Tricine-SDS-PAGE was done essentially as described (27). After SDS-PAGE on an 8.0% polyacrylamide/0.25% bisacrylamide-tricine gel, the proteins were electrophoretically transferred to PVDF membranes (Immobilon P; Millipore). The electrophoretic transfer was done in a Genie electroblot unit (Idea Scientific Co., Minneapolis, MN). Transfer buffer was composed of 20 mM Tris, 185 mM glycine, and 20% (v/v) methanol. After protein transfer the membrane was blocked with 3% BSA, in PBS (10 mM sodium phosphate, 150 mM NaCl, pH 7.4) containing 0.5% Tween, for 30 min at room temperature. The blots were rinsed once with wash buffer (0.1% BSA in PBS containing 0.5% Tween). The blots were then incubated for 1 hr at room temperature with either MAb 2B10 (0.1× hybridoma supernatant) or MAb 4G9 (1 μ g/ml), followed by three 5-min rinses with wash buffer. The blots were then incubated with ¹²⁵I-goat anti-mouse IgG (Fc specific) in wash buffer for 1 hr, followed by three 5-min rinses with wash buffer. The blots were dried at room temperature. The blots were visualized by autoradiography, and radioactivity in individual bands containing Arnt was counted in a Packard Cobra II γ counter (Packard Instrument Co., Meridian, CT). Total protein in cytosolic and nuclear fractions was determined using the bicinchoninic acid protein assay obtained from Pierce Chemical Co.

Sucrose gradient centrifugation analysis. Aliquots (300 μ l) of unlabeled or radiolabeled Hepa 1c1c7 cytosolic or nuclear extracts were layered on 5.1-ml 10–30% sucrose gradients prepared in MENG buffer plus 150 or 500 mM NaCl. The sealed centrifuge tubes were centrifuged in a Beckman VTi65.2 rotor at 416,000 × *g*_{max} for 135 min. After centrifugation, 200- μ l fractions were collected with an Isco (Lincoln, NE) model 640 density gradient fractionator. After acetone precipitation, cytosolic and nuclear extracts were solubilized in 2× SDS-tricine sample buffer, boiled, and subjected to SDS-PAGE (26). BSA (4.4 S) and catalase (11.3 S) were added to separate sucrose gradients as external sedimentation standards.

Gel permeation chromatography. A Superose 6 prepacked HR 10/30 column (Pharmacia LKB Biotechnology, Uppsala, Sweden) was equilibrated in MENG buffer plus either 150 mM NaCl or 500 mM NaCl, and 200- μ l samples were eluted at 26 ml/hr. Hepa 1c1c7 cytosol (6 mg/ml) was used as a source of Arnt. The applied sample volume was 200 μ l. Standards used to calibrate the gel permeation columns (and their Stokes radii) were thyroglobulin (8.5 nm), apoferritin (6.1 nm), alcohol dehydrogenase (4.5 nm), BSA (3.6 nm), and carbonic anhydrase (2.01 nm). The Stokes radius for each protein standard was calculated from references described (28). Distribution coefficients (*K*_D) were calculated from the elution volume according to the equation $K_D = (V_e - V_0)/(V_t - V_0)$, where *V*_e is the elution volume of the peak, *V*₀ is the void volume of the column as determined with blue dextran (*M*_r ~2 × 10⁶), and *V*_t is the total column volume. The *V*₀ corresponds to fraction 0 in the elution profile in Fig. 4. The Stokes radius (*R*_s) of the

Arnt-containing radioactive bands cut from Western blots of electrophoresed gel permeation fractions was determined graphically from a linear plot of (–log *K*_D)^{1/3} versus *R*_s for the standards in each column. The relative molecular mass of Arnt was calculated according to the method of Seigel and Monty (29), using 4127(*s*_{20,w}, *R*_s), where *s*_{20,w} (sedimentation coefficient) was in Svedberg units, *R*_s was in nanometers, and the factor was based on a partial specific volume of 0.725 cm³/g (28).

Indirect immunofluorescence microscopy. Sterile, poly-L-lysine-coated, HTC-printed microscope slides (Cel-line Associates, Newfield, NJ) were placed in 100-mm sterile culture dishes. Hepa 1c1c7 cells were plated onto 5-mm wells on the slides, at a density of 1 × 10⁴ cells/well, in medium (described above). After 4 hr the slides were covered with 25 ml of complete medium, and cells were grown for 24 hr at 37° in 94% air/6% CO₂. The slides were then rinsed for 1 min in 90 ml of PBS, pH 8.0, and fixed by incubation with 4% paraformaldehyde in PBS for 15 min at room temperature. The fixing solution was washed from the cells with one 2-min rinse in 90 ml of PBS, pH 8.0. Permeabilization was carried out for 2 min in methanol at room temperature. The permeabilization solution was washed off with a 2-min rinse in 90 ml of PBS, pH 8.0. Incubations with primary and secondary antibody preparations were carried out by placing the slides on water-saturated filters in 100-mm culture dishes. Nonspecific binding was blocked by incubating cells with 3% goat serum in PBS. After 1 hr the goat serum was rinsed off with five washes of PBS, pH 8.0. The cells were then incubated with either affinity-purified MAb 4G9, MAb 2B10, control mouse antibodies of identical isotype (IgG1 for 2B10 and 4G9), or no primary antibody. Each antibody was diluted in 1% BSA, 0.05% Tween, 0.02% sodium azide, and slides were incubated with primary antibody for 18–24 hr at 4°. After removal of the antibody solution, the cells were washed five times with PBS, pH 8.0, for a total of 15 min. LRSC-conjugated goat anti-mouse IgG was diluted 1/100 in PBS, pH 8.0, and incubated with the cells for 15 min at room temperature. The cells were then washed using the same protocol as after the primary antibody incubation. The cells were cleared of water using a graded series of three glycerol solutions (70% and 90% glycerol in PBS and 100% glycerol, all with 1% propyl gallate), for a total of 18 hr. The cells were mounted in the residual 100% glycerol/1% propyl gallate solution. Cells were visualized with a Leitz Ortholux II microscope equipped with epifluorescence optics and a Leitz Wetzlar (40/0.65) objective lens. Black-and-white pictures were taken using a Nikon M-35F camera attached to a 23.2× magnification photographic tube and Nikon automatic photometer system, using Kodak TMAX 400 film. Exposure times for negative controls were matched with the exposure times used for the experimental samples.

LSCM. Cells were prepared for LSCM in the manner described above. A Bio-Rad MRC 600 LSCM system equipped with a krypton-argon laser was connected to a Nikon inverted microscope. Digital images were magnified using Bio-Rad software run on an IBM PC XT computer. The *xv* image-analysis program (version 3.0) was run on a Sun Sparcstation 2 computer (Sun Microsystems) to generate digital images. Black-and-white pictures were taken with a 35-mm Kodak camera linked to a Sun Sparcstation 2 computer, using Kodak TMAX 400 film. The confocal microscope, computers, and software used are all the property of the Digital Microscopy and Scientific Visualization Laboratory, Department of Anatomy and Cell Biology, University of Michigan (Ann Arbor, MI).

Results and Discussion

This is the first report describing the production and characterization of two MABs against Arnt, a bHLH-PAS transcription factor that regulates gene transcription in association with the AhR. These antibodies were raised against distinct epitopes on Arnt, to enhance our confidence in the experimental results obtained. The carboxyl-terminal 19 amino acid residues of Arnt were coupled to KLH and used as an immunogen in mice for

MAB production. After screening with an indirect ELISA, 10 clones were obtained and tested on Western blots of COS-2 cytosolic extracts; MAb 2B10 was selected from a group of four MABs exhibiting strong specificity for Arnt, based on superior signal strength and minimal cross-reactivity with other proteins in COS-2 and Hepa 1c1c7 cytosol. A second approach used a chimeric fusion protein, composed of the carboxyl-terminal 378-amino acid Arnt polypeptide linked to staphylococcal Protein A, as an immunogen in mice for MAB production. This approach yielded MAB 4G9, which was found to specifically bind to Arnt in COS-2 and Hepa 1c1c7 cytosolic extracts. Due to its strong immunoreactivity with Arnt on Western blots, MAB 2B10 was deemed most suitable for this assay. In our ELISA to detect MABs to the carboxyl-terminal 19-amino acid Arnt peptide-BSA fusion protein, MAB 4G9 did not cross-react with this peptide (data not shown). This fact suggests that MAB 4G9 interacts with an epitope different from that of MAB 2B10 on Arnt.

We have used human Arnt amino acid sequences as immunogens in mice for the purposes of MAB production. It must be noted that the carboxyl-terminal 19-amino acid human peptide sequence used diverges from the mouse sequence only at amino acid 728 (in the human sequence this amino acid is serine and in the mouse sequence it is threonine).¹ This fact suggests that MAB 2B10 should be equally competent in binding human and murine forms of Arnt. Our results indicate that this approach was successful, due to the strong immunoreactivity of MAB 2B10 with murine Arnt.

The two antibodies obtained by these approaches were initially characterized by Western blot analysis of cytosol obtained from COS-1, COS-2, and Hepa 1c1c7 cells (Figs. 1 and 2). On Western blots of SDS-PAGE gels, each antibody was bound to a single immunoreactive protein, which migrated with an estimated molecular mass of ~87 kDa. No immunoreactive material was detected when the blots were stained with a control mouse IgG fraction. To establish the sensitivity of MAB 2B10, we assessed the ability of this MAB to detect a wide range of Hepa 1c1c7 cytosolic protein concentrations (Fig. 3). The linear relationship between Hepa 1c1c7 cytosolic protein concentration and immunoreactivity (as described in Materials and Methods) confirms the sensitivity of MAB 2B10² and its usefulness in quantitative blotting procedures.

Velocity sedimentation on sucrose gradients and gel permeation chromatography are established methods used to characterize the physicochemical properties of proteins (22, 27). We used Hepa 1c1c7 cytosolic and nuclear extracts as the source of Arnt for velocity sedimentation on sucrose gradients. Using sucrose gradient solutions made from buffers of moderate (150 mM NaCl) and high (500 mM NaCl) ionic strength, Arnt from Hepa 1c1c7 cytosol displayed sedimentation coefficients of 3.6 and 4.1 S, respectively (Fig. 4, A and B). These differ significantly from the published sedimentation coefficients of 9 S, 6 S, and 5 S for the untransformed and transformed AhR complexes and the ligand-binding subunit of the AhR, respectively (14, 20, 22). The sedimentation coefficient of Arnt isolated from nuclear extracts of TCDD-treated Hepa 1c1c7 cells was

estimated to be 6–7 S, which apparently reflects its presence in the transformed AhR complex (Fig. 4C) (14, 19).

Gel permeation chromatography data indicate that Arnt derived from Hepa 1c1c7 cells eluted primarily as a 6.8-nm species (Figs. 5 and 6). This radius did not vary as a function of the ionic strength of the elution buffer (150 mM or 500 mM NaCl). In contrast, the ionic strength of the sucrose gradient solutions accounted for an 0.5 S difference in the sedimentation coefficient of Arnt. This may be a reflection of the relatively low resolution of detection of minor changes in Stokes radii in gel permeation chromatography. Given the large range of Stokes radii among the standards used, small variations may be undetectable. The difference in Stokes radii between the 9 S and 6 S forms of the AhR complex is only 0.4 nm, whereas their relative molecular masses differ by ~100 kDa. From this perspective, results showing identical Stokes radii for Arnt in elution buffers with different ionic strengths are reasonable.

The Stokes radius reported here is identical to that found for the transformed nuclear form of the AhR, which represents the AhR-Arnt heterodimer. Physicochemical evidence indicative of a heterodimer has been reported, with a sedimentation value of 6 S, a Stokes radius of 6.8 nm, and an estimated molecular mass of 176 kDa for the transformed AhR isolated from high-salt nuclear extracts of mouse and rat liver cytosol (14, 20). Estimation of the sedimentation coefficient of Arnt using sucrose gradient sedimentation provides evidence that this 6.8-nm species is not the transformed AhR complex. The sedimentation coefficients of 3.6 and 4.1 S for Arnt from Hepa 1c1c7 cytosol in sucrose gradient solutions containing 150 mM and 500 mM NaCl, respectively, were used, in conjunction with the Stokes radius data, to estimate the relative molecular masses according to the method of Seigel and Monty (28). The molecular masses calculated from these sedimentation coefficients were 101 and 115 kDa, respectively. These data indicate that the Stokes radius of 6.8 nm for Arnt is significantly greater than the Stokes radius of 5 nm for the AhR ligand-binding subunit. Thus, it can be inferred that the larger radius of Arnt is responsible for the radius estimated for the AhR ligand-binding subunit-Arnt heterodimer. This then indicates that heterodimerization results in an alignment of AhR and Arnt in a manner that does not increase the Stokes radius of the heterodimer beyond 6.8 nm.

Estimation of the relative molecular mass of Arnt from its sedimentation coefficients (from 150 and 500 mM NaCl-containing sucrose gradients) and Stokes radius indicates a molecular mass of 101–115 kDa. This molecular mass suggests that Arnt elutes as a monomeric species. This estimated molecular mass differs from the 87-kDa value calculated from the deduced amino acid sequence and the molecular mass estimated from PAGE (7, 12). This "overestimation" of molecular mass, however, is consistent with the estimations of the AhR analyzed under similar conditions. Using similar techniques, the estimated molecular mass of the "dissociated" ligand-binding subunit of the murine AhR ranged from 105 to 118 kDa (22, 30). Other possible explanations for these results are that there is another 20-kDa protein or RNA associated with Arnt.

Indirect immunofluorescence micrography and LSCM were used to study the intracellular localization of Arnt in fixed/permeabilized Hepa 1c1c7, VT{2}, and HeLa cell lines. Results indicated that Arnt localizes to the non-nucleolar portion of the nucleus in control and 1 nM (Hepa 1c1c7 and VT{2} cells)

¹ O. Hankinson, personal communication.

² MAB 4G9 was used exclusively in immunofluorescence assays. It should be noted, however, that MAB 2B10 staining in immunofluorescence assays gave identical, albeit weaker, staining patterns (unpublished observations).

or 10 nM (HeLa cells) TCDD-treated Hepa 1c1c7, VT{2}, and HeLa cells (Figs. 7–9). Using LSCM, a “z-series” [that is, visualization of multiple (10–20) horizontal sections] of scans revealed that Arnt was found in all planes of the non-nucleolar portion of the nucleus in Hepa 1c1c7 cells.³ However, we have not experimentally demonstrated that the regions in the nucleus where the presence of Arnt is excluded are nucleoli. After determination of the subnuclear localization using LSCM, indirect immunofluorescence micrography was used to study VT{2} and HeLa cell lines. These indirect immunofluorescence photomicrographs (Figs. 8 and 9) were of resolution comparable to that of single-section LSCM photomicrographs obtained for Hepa 1c1c7 cells (Fig. 7). It is important to establish that Arnt is localized in the nucleus in a wide variety of cell types and tissues. Indeed, tissue-specific differences in TCDD-mediated signal transduction could be caused by an alteration in the subcellular localization of Arnt. In this study, we have demonstrated the nuclear localization of Arnt in two divergent cell types, i.e., mouse hepatoma and human epithelial tumor cell lines. Pollenz *et al.* (31) recently used polyclonal antibodies against an Arnt fusion protein to establish the localization of Arnt in the non-nucleolar portion of the nucleus of Hepa 1c1c7 cells, using indirect immunofluorescence and immunoelectron microscopy. Like Pollenz and co-workers, we have found Arnt localized in the nucleus of type II (group C) mutants⁴ of Hepa 1c1c7 cells.⁵ Thus, our results are in agreement with the work of those authors and support an updated model of AhR-mediated signal transduction (4, 31). This model holds that ligand-mediated AhR activation to a DNA-binding form, via heterodimerization with Arnt, occurs in the nucleus rather than in the cytoplasm (4). This model is consistent with the subcellular localization of Arnt and sucrose density gradient centrifugation data demonstrating the presence of the 9 S, hsp90-associated AhR complex in the nucleus (19, 21).

To establish the utility of VT{2} cells for studying the effect of Arnt overexpression on AhR-mediated signal transduction, we set out to determine whether the subcellular localization of Arnt was different from that in wild-type Hepa 1c1c7 cells. Despite its being expressed at a 10-fold higher level in VT{2} cells, relative to Hepa 1c1c7 cells,³ the nuclear localization of Arnt was not changed. This may indicate that nuclear localization of Arnt is nonsaturable within the range of Arnt expressed in VT{2} cells. Thus, VT{2} cells provide a valid model for examining the effects of Arnt on AhR-mediated events.

Regulation of intracellular localization may occur through the number and efficiency of the NLS of proteins (23, 32). NLS are generally short stretches of basic amino acids, particularly arginine and lysine. The identification of Arnt as an exclusively nuclear protein suggests that Arnt contains at least one efficient NLS. An amino acid sequence located near the amino terminus of Arnt (amino acids 39–45; Arg-Ala-Ile-Lys-Arg-Arg-Pro) may serve as a NLS (7, 31). The establishment of the nuclear localization of Arnt in a human cell line, as shown here, indicates that its nuclear localization may be conserved across

species. We must await experiments using Arnt NLS deletion mutants to provide definitive evidence of the existence of putative NLS. Because recent work indicates that NLS appear to mediate both nuclear import and export (33, 34), we cannot exclude the possibility that Arnt may facilitate the cytoplasm-nucleus or nucleus-cytoplasm trafficking of the AhR. This is the first report characterizing MABs to distinct epitopes in Arnt. These antibodies should serve as useful tools in the study of AhR-mediated signal transduction. Using these antibodies, we have established the following: 1) the purported cytoplasmic localization of Arnt is an artifact of homogenization, 2) the data presented here support the hypothesis that heterodimerization between Arnt and AhR occurs in the nucleus (4), and 3) velocity sedimentation and gel permeation chromatography data indicate that Arnt exists intracellularly as a monomer. Thus, despite its bHLH-PAS dimerization domains, the majority of Arnt does not appear to be associated with itself (as a homodimer), the AhR, hsp90, or other members of the PAS family of regulatory proteins in Hepa 1c1c7 cytosol in the absence of TCDD. Data presented here support a model wherein AhR activation and transformation to a DNA-binding heterodimer occur in the nucleus, as suggested by others (4, 31). This model differs from a model of AhR activation and dimerization in the cytoplasm before nuclear translocation of the AhR-Arnt heterodimer, as proposed by Hankinson and co-workers (1).

Acknowledgments

We would like to thank Drs. Oliver Hankinson and Herminio Reyes of the University of California, Los Angeles, Medical Center for providing the VT{2} cells, COS cell extracts, and Arnt fusion proteins. We also thank Dr. Mike Welsh and Walter Meixner of the Digital Microscopy and Scientific Visualization Facility in the Department of Anatomy and Cell Biology, University of Michigan Medical School.

References

1. Probst, M. R., S. Reisz-Porszasz, R. V. Agbunag, M. S. Ong, and O. Hankinson. Role of the aryl hydrocarbon receptor nuclear translocator protein in aryl hydrocarbon (dioxin) receptor action. *Mol. Pharmacol.* 44:511–518 (1993).
2. Burbach, K. M., A. Poland, and C. A. Bradfield. Cloning of the Ah-receptor cDNA reveals a distinctive ligand-activated transcription factor. *Proc. Natl. Acad. Sci. USA* 89:8185–8189 (1992).
3. Elferink, C. J., T. A. Gasiewicz, and J. P. Whitlock, Jr. Protein-DNA interactions at a dioxin-responsive enhancer: evidence that the transformed Ah receptor is heteromeric. *J. Biol. Chem.* 265:20708–20712 (1990).
4. Swanson, H. I., and C. A. Bradfield. The Ah-receptor: genetics, structure and function. *Pharmacogenetics* 3:213–230 (1993).
5. Vanden Heuvel, J. P., and G. Lucier. Environmental toxicology of polychlorinated dibenzo-p-dioxins and polychlorinated dibenzofurans. *Environ. Health Perspect.* 100:189–200 (1993).
6. Huang, Z. J., I. Edery, and M. Rosbash. PAS is a dimerization domain common to *Drosophila* Period and several transcription factors. *Nature (Lond.)* 364:259–262 (1993).
7. Reyes, H., S. Reisz-Porszasz, and O. Hankinson. Identification of the Ah receptor nuclear translocator (Arnt) as a component of the DNA binding form of the Ah receptor. *Science (Washington D. C.)* 256:1193–1195 (1992).
8. Crews, S. T., J. B. Thomas, and C. S. Goodman. The *Drosophila* single-minded gene encodes a nuclear protein with sequence similarity to the *per* gene product. *Cell* 52:143–151 (1988).
9. Dolwick, K. M., J. V. Schmidt, L. A. Carver, H. I. Swanson, and C. A. Bradfield. Cloning and expression of the human Ah receptor cDNA. *Mol. Pharmacol.* 44:911–917 (1993).
10. Nambu, J. R., R. G. Franks, S. Hu, and S. T. Crews. The single-minded gene of *Drosophila* is required for the expression of genes important for the development of CNS midline development. *Cell* 63:63–75 (1990).
11. Takahashi, J. S. Circadian clock genes are ticking. *Science (Washington D. C.)* 258:238–240 (1992).
12. Hoffman, E. C., H. Reyes, F. F. Chu, F. Sander, L. H. Conley, B. A. Brooks, and O. Hankinson. Cloning of a factor required for activity of the Ah (dioxin) receptor. *Science (Washington D. C.)* 252:954–958 (1991).
13. Perdew, G. H. Chemical cross-linking of the cytosolic and nuclear forms of the Ah receptor in hepatoma cell line 1c1c7. *Biochem. Biophys. Res. Commun.* 182:55–62 (1992).

³ N. G. Hord, S. S. Singh, and G. H. Perdew, unpublished observations.

⁴ Type II (group C) variants contain the same level of AhR and identical agonist affinity, compared with wild-type Hepa 1c1c7 cells. However, AhR cannot be recovered in the nuclear fraction after TCDD treatment. This defect has been attributed to defective Arnt function, due to the fact that transfection of group C mutants with a human Arnt expression vector partially restores TCDD-mediated AhR nuclear uptake (12).

⁵ N. G. Hord, S. S. Singh, and G. H. Perdew, unpublished observations.

14. Prokipcak, R. D., and A. B. Okey. Physicochemical characterization of the nuclear form of Ah receptor from mouse hepatoma cells exposed in culture to TCDD. *Arch. Biochem. Biophys.* **267**:811–828 (1988).
15. Perdew, G. H. Association of the Ah receptor with the 90-kDa heat shock protein. *J. Biol. Chem.* **263**:13802–13805 (1988).
16. Whitelaw, M., I. Pongratz, A. Wilhelmsson, J.-A. Gustafsson, and L. Poellinger. Ligand-dependent recruitment of the Arnt coregulator determines DNA recognition by the dioxin receptor. *Mol. Cell. Biol.* **13**:2504–2514 (1993).
17. Pongratz, I., G. Mason, and L. Poellinger. Dual roles of the 90 kDa heat shock protein hsp90 in modulating functional activities of the dioxin receptor. *J. Biol. Chem.* **267**:13728–13734 (1992).
18. Hankinson, O. Research on the aryl hydrocarbon (dioxin) receptor is primed to take off. *Arch. Biochem. Biophys.* **300**:1–5 (1993).
19. Perdew, G. H. Comparison of the nuclear and cytosolic forms of the Ah receptor from Hepa 1c1c7 cells: charge heterogeneity and ATP-binding properties. *Arch. Biochem. Biophys.* **291**:284–290 (1991).
20. Cuthill, S., L. Poellinger, and J.-A. Gustafsson. The receptor for 2,3,7,8-tetrachlorodibenzo-*p*-dioxin in the mouse hepatoma cell line Hepa 1c1c7. *J. Biol. Chem.* **262**:3477–3481 (1987).
21. Wilhelmsson, A., S. Cuthill, M. Denis, A.-C. Wikstrom, J.-A. Gustafsson, and L. Poellinger. The specific DNA binding activity of the dioxin receptor is modulated by the 90 kD heat shock protein. *EMBO J.* **9**:69–76 (1990).
22. Denslow, M. S., L. M. Vella, and A. B. Okey. Structure and function of the Ah receptor for 2,3,7,8-tetrachlorodibenzo-*p*-dioxin. *J. Biol. Chem.* **261**:3987–3995 (1986).
23. Guiochon-Mantel, A., and D. Milgrom. Cytoplasmic-nuclear trafficking of steroid hormone receptors. *Trends Endocrinol. Metab.* **4**:322–328 (1993).
24. Markwell, M. A. K. A new solid-state reagent to iodinate proteins. *Anal. Biochem.* **125**:427–432 (1982).
25. Bernatowicz, M. S., and G. R. Matsuada. Preparation of peptide-protein immunogens using *N*-succinimidyl bromoacetate as a heterobifunctional cross-linking reagent. *Anal. Biochem.* **155**:95–102 (1986).
26. Ross, A. H., D. Herlyn, and H. Koprowski. Purification of monoclonal antibodies from ascites using ABx liquid chromatography column. *J. Immunol. Methods* **102**:227–231 (1987).
27. Schagger, H., and G. von Jagow. Tricine-sodium dodecyl sulfate-polyacrylamide gel electrophoresis for the separation of proteins in the range from 1 to 100 kDa. *Anal. Biochem.* **166**:368–379 (1987).
28. Seigel, L. M., and K. J. Monty. Determination of molecular weights and frictional ratios of proteins in impure systems by use of gel filtration and density gradient centrifugation: application to crude preparations of sulfite and hydroxylamine reductases. *Biochim. Biophys. Acta* **112**:346–36 (1966).
29. Sherman, M. R. Cytoplasmic receptors for steroid hormones. *Methods Enzymol.* **36**:211–234 (1975).
30. Piskorska-Pliszczynska, J., and S. Safe. Radioligand-dependent differences in the molecular properties of the mouse and rat hepatic aryl hydrocarbon receptor complexes. *Arch. Biochem. Biophys.* **267**:372–383 (1988).
31. Pollenz, R. S., C. A. Sattler, and A. Poland. The aryl hydrocarbon receptor and aryl hydrocarbon receptor nuclear translocator protein show distinct subcellular localizations in Hepa 1c1c7 cells by immunofluorescence microscopy. *Mol. Pharmacol.* **45**:428–438 (1994).
32. Silver, P., and H. Goodson. Nuclear protein transport. *Crit. Rev. Biochem. Mol. Biol.* **24**:419–435 (1989).
33. Guiochon-Mantel, A., K. Delabre, P. Lescop, M. Perrot-Appianat, and E. Milgrom. Cytoplasmic-nuclear shuttling trafficking of progesterone receptor. *Biochem. Pharmacol.* **47**:21–24 (1994).
34. Mandell, R. B., and D. M. Feldherr. Identification of two HSP70-related *Xenopus* oocyte proteins that are capable of recycling across the nuclear envelope. *J. Cell Biol.* **111**:1775–1783 (1990).

Send reprint requests to: Gary Perdew, Department of Foods and Nutrition, Stone Hall, Purdue University, West Lafayette, IN 47904.
